

Energy & Environmental Science

Accepted Manuscript



This is an *Accepted Manuscript*, which has been through the Royal Society of Chemistry peer review process and has been accepted for publication.

Accepted Manuscripts are published online shortly after acceptance, before technical editing, formatting and proof reading. Using this free service, authors can make their results available to the community, in citable form, before we publish the edited article. We will replace this *Accepted Manuscript* with the edited and formatted *Advance Article* as soon as it is available.

You can find more information about *Accepted Manuscripts* in the [Information for Authors](#).

Please note that technical editing may introduce minor changes to the text and/or graphics, which may alter content. The journal's standard [Terms & Conditions](#) and the [Ethical guidelines](#) still apply. In no event shall the Royal Society of Chemistry be held responsible for any errors or omissions in this *Accepted Manuscript* or any consequences arising from the use of any information it contains.

Corn protein-derived nitrogen-doped carbon materials with oxygen-rich functional groups: A highly efficient electrocatalyst for the all-vanadium redox flow batteries †

Cite this: DOI: 10.1039/x0xx00000x

Received 00th January 2012,
Accepted 00th January 2012

DOI: 10.1039/x0xx00000x

www.rsc.org/

Minjoon Park, Jaechan Ryu, Youngsik Kim and Jaephil Cho *

Recent studies for all-vanadium redox flow batteries (VRFBs) have been focused on carbon-based materials for cost-effective electrocatalysts to commercialize them in grid-scale energy storage markets. We report an environmentally friendly and safe method for carbon-based catalysts by a corn protein self-assembly. This new method allows the carbon black nanoparticles to be coated with nitrogen-doped graphitic layers with oxygen-rich functionalities (N-CB). We observed the increased catalytic activity of this catalyst toward both V^{2+}/V^{3+} and VO^{2+}/VO_2^+ ions, showing the 24 % increased mass transfer process and ca. 50 mV higher reduction onset potential comparing to CB catalyst. It is believed that the abundant oxygen active sites and nitrogen defects of the N-CB catalyst are beneficial to the vanadium redox reaction by improving electron transfer rate and faster vanadium ion transfer kinetics.

Broader context

All-vanadium redox flow batteries has received great attention as a possible solution for the large-scale energy storage system (ESS), which is first invented by M. Skyllas Kazacos in 1985. This system has several advantages such as a long cycle life, design flexibility, and safety etc., however, the low energy density, and poor reactivity on carbon materials are a great obstacle in market penetration. We used the corn protein, “zein” as a nitrogen doping source, which has been produced by the Unites States as a leading producer for a long period, left behind as a byproduct after the manufacture of corn flour, corn oil, and bio-ethanol and so forth. This study presents that the highly effective corn protein-derived nitrogen-doped carbon materials with oxygen-rich electrocatalyst can be achieved by the safe and low-cost method. Thus, this technology with cost-effective and scalable properties are greatly important for its application in grid-scale energy storage systems. In addition, the application of corn protein as the heteroatom doping sources will be readily adaptable for other electrode materials applied to various battery systems.

Introduction

In recent years, the rechargeable grid-scale energy storage systems (ESS) such as the redox flow batteries coupled with renewable energy sources have been attracted to solve daily and seasonal problems, for instance, intermittency, nonlinearity and uncertainty of power input and output.^{1,2} Out of various redox flow batteries such as lithium iodine redox battery³ or organic-inorganic redox flow battery,⁴ the all-vanadium redox flow batteries (VRFBs) have been widely studied and successfully

deployed on a commercial scale.⁵ The VRFBs has several advantages such as a decoupling of energy and capacity and long cycle life. In contrast to conventional lithium ion battery's electrodes that store energy-bearing species in their interstitial structures, the electrodes of the VRFBs only provide the redox active surface (sites) for the redox reaction without changing their structure, phase, and morphology, where vanadium redox reactions occur on the electrode surface. For this reason, the longer service life of the electrode can be expected in VRFBs.

In spite of several advantages, the increase of overall cell polarization at a higher charge/discharge current density during cycles in flow cells is a critical issue to attain a high rate capability and high efficiency. The overpotentials in flow cell systems consist of ohmic polarization, charge transfer polarization, and concentration polarization resistance.⁶ Bin Li et al. reported the electrode material and its surface chemistry

School of Energy and Chemical Engineering, Ulsan National Institute of Science and Technology (UNIST), Ulsan, 689-798, South Korea. E-mail: jpcho@unist.ac.kr

† Electronic Supplementary Information (ESI) available: Table S1, and Figure S1–S9. See DOI: 10.1039/b000000x/

determine the system polarization such as a charge transfer resistance, because the vanadium redox reaction takes place on the electrode surface.⁷ They also reported that overpotentials arising from concentration polarizations remain the same, since identical electrolytes, membranes, and flow rates are used in the flow cell test. Thus, many researchers have focused on the reduction of cell overpotentials in flow cells by developing effective electrode materials and electrocatalysts.

A carbon-based material such as pristine carbon felts has been considered as the one of the most promising electrode material for VRFBs due to its low-cost, high stability, high conductivity, and corrosion resistance.^{7, 8} However, its poor kinetic reversibility and electrochemical reactivity hampered the commercialization of the VRFBs with a low current density during the charge/discharge cycles.^{9, 10} Over the years, intensive efforts have been devoted to overcome the above-mentioned drawbacks by introducing surface functionalities for abundant active sites or increasing electron conductivities.¹¹ To better understand the state-of-the art of various electrocatalysts in the VRFB systems, recent studies are summarized, presenting electrochemical properties with various current densities and cycles (Supporting Information, Table S1).¹²⁻¹⁷

The metal-based catalysts (Pt,¹⁸ Bi,¹⁹ and Ir¹⁷ etc.) deposited onto the carbon felt has been studied to improve the cycle performance and catalytic activity for the vanadium redox reaction. However, this approach has been discouraged because of their scarcity of metals or sensitivity to gas evolutions. Recently, Pacific Northwest National Laboratory (PNNL) has reported several novel catalysts with low cost, excellent stability, and cell performance by using a bismuth nanoparticle or niobium oxide nanorod.^{7, 20} As an alternative strategy, modified carbon materials have been studied as an effective candidate for further wide applications of the VRFBs.²¹ Recently, we reported on the use of the CNT/CNF composite as a carbon-based electrocatalyst, which led to outstanding cell performance.²² Significantly, N-doping into carbon materials, including CNTs,¹⁴ graphene,²³ and mesoporous carbon²⁴ have been found to improve the vanadium redox reaction by facilitating the formation of defects sites for ion adsorptions. On the other hand, the difficulty of their synthesis processes involved in a toxicity of ammonia, high price of metal precursor, or flammability of ethylenediamine at higher temperatures hindered their mass productions. This has been one of the critical issues for the commercial uptake of the VRFBs. Bio-derived heteroatom-doped carbon materials have been widely studied as electrode/catalyst materials for energy devices.²⁵⁻²⁹ Recently, to overcome these drawbacks, various amino acids such as alanine, cysteine, and glycine has been studied as a safe, non-toxic and inexpensive heteroatom doping source for electrocatalysts.³⁰

We proposed a new synthesis process for highly active carbon-based electrocatalysts by using a corn protein, "Zein". The zein is a major protein of corns that has been massively produced in United States at a low cost (\$10/kg).^{31, 32} The composition of zein protein can be classified by 50% hydrophobic amino acids including alanine, proline and leucine, providing a nitrogen for growing kernels (Figure S1). This material mainly contains a high α -helix content with β -sheet fractions.³³ In addition, the zein molecules has a unique structure with amphiphilic characteristics,^{34, 35} which is one of the main driving force to form ordered-film structures without external actions and their self-organization into two-dimensional periodic structures.³⁶

In this work, inspired by previous researches on the zein self-assembly, bio-derived nitrogen-doped carbon black particles, denoted as the N-CB catalyst, were fabricated, which has abundant oxygen active sites and nitrogen defects for vanadium redox reactions. Without supplying any external nitrogen containing gases or metal seeds, the rearrangement of zein molecules and film forming behavior facilitated the formation of the heteroatom doping on the surface of the CB particles. It was first time to utilize the corn protein as a doping source and to prepare nitrogen-doped carbon materials by zein self-assembly, to the best our knowledge.

Experimental

Catalyst design and Catalyst synthesis

The N-CB catalyst was made by the simple solution method involving the evaporation-induced self-assembly process (EISA) in binary solvents. First, 0.1 g of the zein powders (Zein, Sigma Aldrich) were stirred in the mixed solvent composed of 7 mL of ethanol and 3 mL of DI water, and then the yellow colored zein solution was obtained after 10 minutes of stirring. The zein solution was blended with 0.3 g of carbon black (Ketjen black, EC-600JD, AkzoNobel) particles, resulting in formation of the zein coated on the carbon black composite. In addition, the various compositions of the zein and carbon black powders (1:1, 1:3, 2:3, 1:8, and 1:15) were prepared at 800 °C in Ar to find the optimized condition. The selected composition is 1:3 the ratio according to the electrochemical results as shown in Figure S7. This binary solvent was evaporated at 60 °C to allow the zein to have self-assembly on the CB surface by forming zein thin films. Next, the remaining powders were placed on tube furnace and fired for 3 h at various temperatures (700, 800, and 900 °C) in Ar atmosphere. Finally, the N-CB catalyst composites were obtained after the furnace cooled down to the room temperatures. For comparison, the pristine carbon black was also heat-treated above-mentioned temperatures as a control sample.

Electrochemical measurements

The cyclic voltammetry were measured using a typical three-electrode cell. The carbon felt as a working electrode with a diameter of 6 mm was connected to a platinum wire with a reference electrode (Ag/AgCl), and counter electrode (Pt wire) in 0.1 M VOSO₄ (Sigma-Aldrich, 99.5%) in 3 M H₂SO₄ solution (Sigma-Aldrich, 98%) at a different scan rate ranged from 1 to 10 mV s⁻¹. A single cell was assembled for charge/discharge tests (Supplementary Information, Figure S8). The positive electrolyte was prepared by dissolving 2 M VOSO₄ in 3 M H₂SO₄ solution. The negative electrolyte was also prepared by electrolysis of 2 M VOSO₄ in 3 M H₂SO₄ solution, then 20 mL of positive and negative electrolyte was used at charge/discharge test, respectively. The untreated and prepared electrodes with (an active area of 5 cm²) with a thickness of 3 mm were used as the positive and negative electrode, respectively, and compressed into a thickness of 2 mm when stacking electrodes. Nafion117 ion exchange membrane was employed and graphite-based plate was placed between electrode and copper current collectors. The test cell was charged and discharged under the operating potential range of 1.65 to 0.8 V with a current density range of 50 mA cm⁻² to 150 mA cm⁻² and a flow rate of 50 mL min⁻¹.

Characterization

SEM and TEM images were taken using FE-SEM (S-4800, Hitachi) operating at 10 kV and HR-TEM (JEM2100, JEOL) operating at 200 kV, respectively. Elemental mapping was attained using energy-dispersive X-ray spectroscopy equipped in the TEM. XRD pattern was obtained on an X-ray diffractometer (D/Max2000, Rigaku). Surface chemistry was examined by X-ray photoelectron spectroscopy (Thermo Fisher, UK). Raman spectra were collected on a Micro-Raman (WITec) with 532 nm lasers. BET measurement was used to determine the specific surface area of electrodes (ASAP2420, Micromeritics). A potentiostat/galvanostat (WBC3000, WonAtech) was used to evaluate the electrochemical properties. Electrochemical impedance spectrum (EIS) was measured on single potentiostat (Ivium) by applying an alternating voltage of 5 mV over the frequency ranging from 10^{-2} to 105 Hz.

Electrode fabrication

The N-CB carbon felt electrode was made by coating the prepared the catalyst on the carbon felt (PAN CF-20-3, Nippon carbon) surface and drying at 60 °C. First, the N-CB catalyst ink was prepared by dissolving 20 mg of the N-CB particles in the mixture of 100 μ l of 5 wt% Nafion (Sigma-Aldrich), and 900 μ l of ethanol, then followed by ultrasonically blending for 20 min. The CB catalyst ink was fabricated by identical process. The 5 mg cm^{-2} of catalyst ink was coated onto a carbon felt to provide the distributed catalyst layer, and then dried at 60 °C for 12 h. The 5 cm^{-2} of electrodes were equipped in a single cell at both negative and positive side for charge/discharge cycling tests.

Results and discussion

The effective active site for the redox reaction of vanadium ions and excellent electron conductivity of the electrode are the key parameters to the increase in mass transfer rate and electron transfer kinetics toward vanadium redox couples.²³ To promote the electrochemical properties of the electrode, we coated the carbon black with the zein protein via the evaporation-induced self-assembly method (EISA).³⁶ After carbonization of the zein in an inert atmosphere (Figure 1a), it can provide more effective oxygen-rich active sites for the vanadium redox reaction, and develop electron conductive networks by forming nitrogen-doped layer. This functionalized coating layer can be contributed to the improvement of cell performance by improving the vanadium redox reaction during the charge and discharge at high current rates.

The synthesis process of oxygen-rich and nitrogen-doped coating layer on CB using the zein self-assembly is environmentally friendly, simple and highly scalable. Briefly, the N-CB catalyst was prepared by a simple solution method involving the EISA method in binary solvents, followed by a heat treatment (see Experimental section for a detailed description). The zein powder was dissolved in mixed solvent composed of 7 mL ethanol and 3 mL DI water, then a yellow colored zein solution was obtained after 10 minutes (Figure 1b). This solution was blended with the carbon black particles to treat them under the EISA process, resulting in zein-coated carbon black powders. Consequently, the binary solvent was evaporated at 60 °C, followed by firing it in a tube furnace at 800 °C for 3 h in Ar gas. Finally, the prepared N-CB catalyst was coated on a carbon felt substrate and then dried to form a uniform catalyst layer loading of 5 mg cm^{-2} .

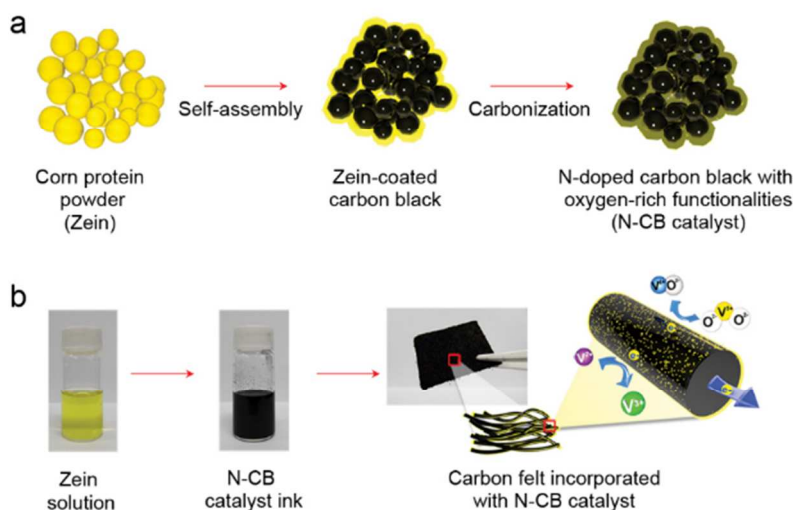


Figure 1. a) Schematic of the N-CB catalyst fabrication process. b) The zein powder was dissolved in a binary solvent, then the CB was immersed in the solution. As the solution was evaporated at an oven, a self-assembly of zein on the CB was proceeded. The dried powders were converted into the N-CB catalyst by a carbonization at 800 °C in argon atmosphere, then the catalyst ink was prepared by blending the N-CB in Nafion suspensions in ethanol. Finally, a carbon felt was coated with the N-CB catalyst by using the prepared ink.

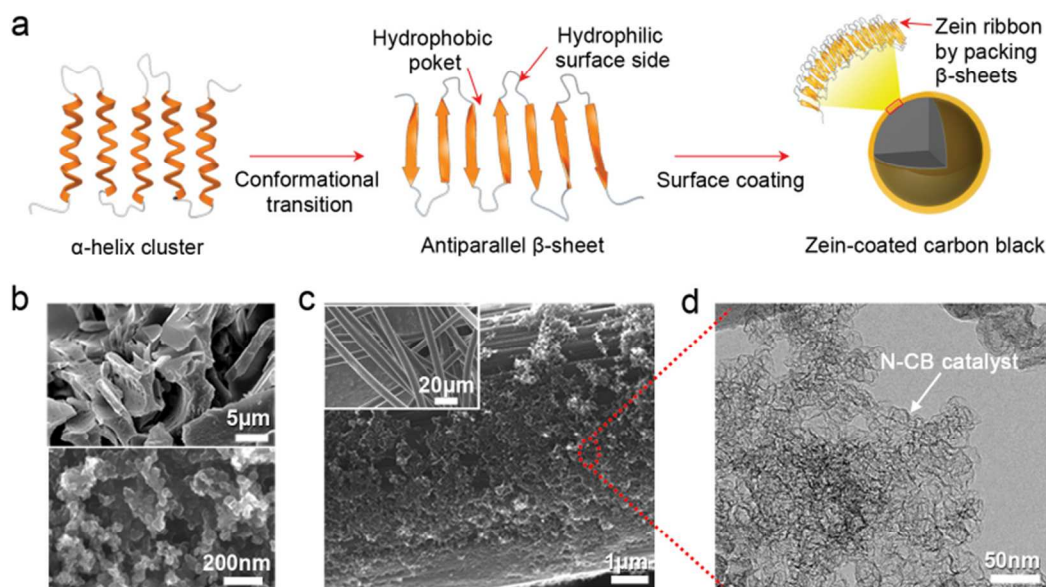


Figure 2. a) Possible mechanism for the self-assembly of the zein coated CB nanoparticles. b) SEM image of the pristine zein powders (upper) and the pristine CB nanoparticles (lower). c) SEM image of the carbon felt surface coated with the N-CB catalyst. Inset image of the untreated carbon felt. d) HR-TEM image of the N-CB catalyst.

The mechanism of forming a self-assembled zein film on the carbon black particles was presented in Figure 2a. The molecular structure of the zein have been studied previously, presenting its single molecule dissolved in ethanol/water consists of ca. 80% of the α -helix at an initial stage.³⁶ The content of the α -helix in solvents could be controlled by controlling the concentration of solutes and the volume ratio of solvents. The β -sheet transformed from the α -helix could be arranged by controlling an evaporation rate of the binary solvents during the EISA process. This led to the change of a solvent polarity by the hydrophilic condition, which drove the self-assembly of zein molecules. Wang and Padua reported that the nano-sized zein sphere, hexagonal, and lamellar phases were formed by packing an energetically favorable β -sheet structure. It was presented by TEM images where antiparallel β -sheets were packed side by side to form long ribbons with a periodic distance of 0.35 nm.³⁶ Finally, the carbon black nanoparticles could be coated by the zein ribbons interacted with the β -sheets, then followed by the carbonization treatment to obtain the N-doped CB particles.

Figure 2b presents the scanning electron microscopy (SEM) images of the pristine zein powder (upper) and untreated CB particles (lower). Typically, the CB nanoparticles have a mesoporous structure with an average diameter of ~ 50 nm, which can facilitate the vanadium ion adsorption by providing

large active sites. As presented in Figure 2c, the N-CB catalyst was successfully coated on the carbon felt surface (inset image: untreated carbon felt surface with a diameter ~ 7 μm). The N-CB catalyst was well distributed on the carbon felt as observed in magnified SEM image (dashed circle in Figure 2c). HR-TEM image of the N-CB catalyst shows each CB nanoparticles are aggregated by the functionalized graphitic layers (Figure 2d). The magnified image of Figure 2d presents the defective graphitic surface with 0.34 nm spacing between adjacent lattice planes (Figure S2b). As a result, the surface morphology of N-CB catalyst was not significantly changed when treated by zein protein (Figure S2). The specific surface area of the N-CB catalyst was also measured in the value of ca. $984.5 \text{ m}^2 \text{ g}^{-1}$ (Figure S3). It believed that N-CB catalyst can sufficiently contribute to the better electrochemical performance with large surface areas. The change of the surface chemistry will be examined by EDXS, XPS and Raman analysis. Energy dispersed X-ray spectroscopy (EDXS) showed that the oxygen and nitrogen atoms were successfully incorporated into the N-CB particles, which could act as highly reactive active sites for vanadium redox couples (Figure S4). Raman spectroscopy was also conducted to further study the microstructure of the obtained samples (Figure 3). The peaks at 1340 cm^{-1} and 1590 cm^{-1} correspond to the D and G bands of typical carbon materials.³⁷ In the first-order region of two strong bands, the intensity of the defect-induced D band is much higher than that of the G band, indicating that there were relatively abundant exposed-graphitic defects that can serve as the redox active sites in both carbon black and the N-CB samples. However, the higher D/G intensity ratio was observed in the N-CB catalyst due to the oxygen-rich functional groups and more defective N-doped layers. This imply that the oxygen and nitrogen functionalities could facilitate the formation of reactive defect sites for vanadium redox ions.³⁸

X-ray photoelectron spectroscopy (XPS) analysis (Figure 4) indicated the presence and the chemical structures of oxygen and nitrogen atoms on the surface of the catalyst samples,

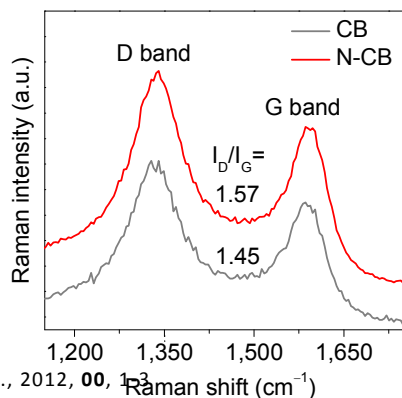


Figure 3. Raman spectroscopy of the CB and N-CB catalyst.

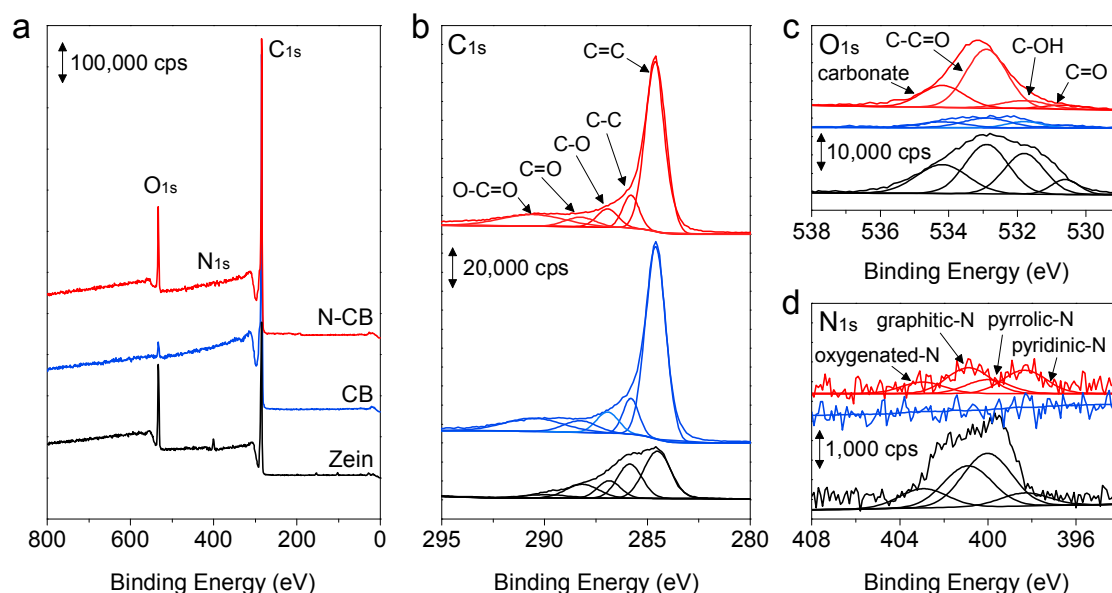


Figure 4. a) XPS survey of the pristine zein, CB, and N-CB catalyst. XPS analysis and its fitting from high resolution b) C1s peak, c) O1s peak, and d) N1s peak.

where all spectra were calibrated by the C1s peak of carbon at 284.2 eV. The chemical composition ratio of each functional group was also presented in Figure S5. For the N-CB sample, the XPS survey presents a predominant C1s signal with a much stronger O1s peak at 531 eV, arising from oxygen-containing species in the zein molecules than that of untreated CB. The high-resolution C1s spectrum of the pristine zein shows a relatively weak energy intensity of the double-bonded carbon peak, while the corresponding high-resolution C1s spectrum observed in the untreated CB and N-CB catalyst exhibits a sharp graphitic carbon peak at 284.2 eV (Figure 4b). As shown in Figure 4c, the O1s peaks of the N-CB catalyst assigned to 532.9, 531.8, and 530.6 eV can be attributed to C-C=O, C-OH, and C=O, respectively,³⁹ indicating the increased incorporation of oxygen functional groups on the carbon black surface. They can act as the main active sites for vanadium redox couples. More specifically, the content of the C-C=O functional group of the N-CB sample, which is directly associated with vanadium redox sites, was increased in more than 27% when compared to that of the CB sample. As shown in Figure 4d, no significant signals were found in the N1s region in the untreated CB sample, while the nitrogen-containing groups on the N-CB sample were observed with a noticeable increase of N1s signal at 400 eV. The nitrogen content in the N-CB catalyst was 1.62 at% according to XPS analysis. The N1s region can be deconvoluted into four peaks assignable to the oxygenated-N (402.9 eV), graphitic-N (401.1 eV), pyrrolic-N (400.0 eV), and pyridinic-N (398.3 eV), respectively (Figure 4d).⁴⁰ These nitrogen species in the carbon materials have been known to produce the defects in the graphite layer, contributing to the improvement of the catalytic activity toward vanadium ions.²³ Thus, the N-doping defects in the N-CB catalyst can serve as an important role in vanadium redox reactions by forming the vanadium ions adsorption sites.

Cyclic voltammetry tests were performed on the three-electrode cell system to characterize the electrochemical properties of the N-CB catalyst. The test cell was composed of negative and positive vanadium electrolytes in which carbon felt electrode, platinum wire, and Ag/AgCl were used as

working, counter, and reference electrodes, respectively (detailed in Experimental section). There are several parameters that can estimate catalytic activities for vanadium redox reactions, for instance the potential separation (ΔV), the ratio of oxidation and reduction peak current (I_{pa}/I_{pc}), and the redox onset potential. As shown in Figure 5a, the redox potential separation of the oxidized carbon felt (OCF) electrode ($\Delta V=353$ mV) is substantially larger than that of CB-CF one ($\Delta V=195$ mV), implying that it has poor electrochemical reversibility. As for the ratio of the redox peak current (I_{pa}/I_{pc}), the OCF electrode ($I_{pa}/I_{pc}=1.54$) presents unstable vanadium redox reaction compared to CB-CF electrode ($I_{pa}/I_{pc}=1.10$). The onset redox potential of CB-CF also present much better than that of OCF electrode. We used the N-CB catalyst that heat-treated at 800 °C as the optimized working electrode because it exhibited the best anodic and cathodic peak current density ($i_{pa} = 86.3$ and $i_{pc} = -75.1$ mA cm⁻²) and lowest onset potential (See Figure S7b). As shown in Figure 5a, the pronounced redox peaks corresponding to the oxidation and reduction of VO²⁺ and VO₂⁺ ions presented in the cyclic voltammograms. These peaks appeared in the carbon felt coated with the CB or N-CB samples, while the weak reduction peak at 0.75 V (vs. Ag/AgCl) is observed in the untreated carbon felt. Significantly, the reduction onset potential measured from the N-CB carbon felt electrode was around 50 mV higher than that of the CB carbon felt sample (Figure 5a, inset). This suggests that the improved catalytic activity is originated from the N-CB catalyst. Furthermore, the peak potential separation associated with the polarization of the N-CB carbon felt electrode was decreased to 146 mV at a scan rate of 5 mV s⁻¹. This implies the enhanced reversibility for vanadium redox reactions. As for the negative redox reaction involving V²⁺/V³⁺ ions, the distinct anodic and cathodic peaks of the N-CB carbon felt were observed at -0.21 V and -0.71 V (vs. Ag/AgCl), respectively, while there were no pronounced anodic and cathodic peaks for the untreated carbon felt electrode (Figure S6). When the cyclic voltammogram of each sample were compared, the onset potential and potential separation of the N-CB carbon felt were much lower than those of the CB carbon felt at both negative

and positive vanadium redox reactions. This improved electrochemical behavior can be caused by improved electron transfer and sufficient vanadium redox active sites owing to oxygen-rich and nitrogen-doped graphitic layers. The electrochemical impedance spectroscopy (EIS) analysis also agreed with the results of the cyclic voltammetry tests, suggesting that the formation of electrically conductive network introduced by functionalized graphitic layer could reduce the electron transfer resistance by ca. 26% (Figure S6d).

The mass transfer properties can be assessed by plotting the peak current density versus the square root of scan rate from the Randles-Sevcik equation.⁴¹ Figures 5b and c show the cyclic voltammetry tests, which were conducted as increasing scan rates from 1 mV s⁻¹ to 10 mV s⁻¹ in 0.1 M VOSO₄ + 3 M H₂SO₄ solutions. The value of coefficient of determination (R^2)

inserted in Figure 5c was close to 99%, implying that a diffusion process controls the vanadium redox reaction on the N-CB carbon felt electrode. In addition, the slope of the N-CB carbon felt electrode (Figure 5b) is 24% larger than that of the CB carbon felt electrode, suggesting that a faster mass transfer process could be achieved on the N-CB carbon felt electrode. The improved mass transfer reaction on the N-CB catalyst could be ascribed to its high electrochemical surface areas and lower surface energy induced by the heteroatom doped coating layer.

To demonstrate the practical application of the prepared catalyst, we used the carbon felt electrode incorporated with the N-CB catalyst as the negative and positive electrodes in all-vanadium redox flow battery. We assembled flow-type single cells to evaluate the electrochemical performances of the untreated, CB, and N-CB carbon felt electrode. The cell body was assembled by using Nafion 117 (the proton exchange membrane), copper plates (the current collectors) and graphite-based bipolar plate that protect current collectors from acidic electrolytes (detailed in Figure S8 and Experimental section). Electrolytes consisting of 20 mL of 2 M V³⁺ and 20 mL of V⁴⁺ based on 3 M H₂SO₄ solutions were used as the negative and positive electrolytes, respectively.

Figures 6a and b show the voltage profiles of the CB carbon felt and N-CB carbon felt electrode, respectively, between 0.8 and 1.65 V at various charge/discharge current densities. The N-CB carbon felt electrode presented improved discharge capacity of 19.2 and 10.1 Ah L⁻¹ at the current density of 50 and 150 mA cm⁻², respectively (see Figure 7b). Additionally, the N-CB catalyst exhibited stable cycling performance for 100 cycles at 50 mA cm⁻² as depicted in Figure 6c. This catalyst also presented the energy efficiency (Coulombic efficiency × Voltage efficiency) of 85.2% at the end of 100 cycles corresponding to 450 h (4.5 h per cycles). The coulombic efficiency is the difference between the charge and discharge capacity. Likewise, the voltage efficiency is the ratio of charge and discharge voltage. After the initial charge/discharge rate of 50 mA cm⁻² for 5 cycles, we gradually increased the current density to 150 mA cm⁻². The N-CB carbon felt electrode showed the energy efficiency of 86.7% at 50 mA cm⁻² and 68.6% at the rate of 150 mA cm⁻². The origin of the enhanced rate capability for the N-CB catalyst during battery cycling can be possibly attributed to the significantly reduced polarizations by increased redox active sites towards vanadium ions for the fast electron and mass transfer reactions. Next, to evaluate the stability of the N-CB catalyst, we swiftly changed the charge/discharge rate from 150 to 50 mA cm⁻² (Figure 6c). Notably, the initial energy efficiency was remarkably recovered. This indicates the electrochemical and chemical robustness of the N-CB catalyst in concentrated acidic vanadium electrolytes. As shown in Figure S9, we also confirmed the stable adhesion of N-CB catalyst on carbon felt electrode after 100 cycles. The coulombic efficiency and voltage efficiency values also showed the best in N-CB samples, as shown in Figure 6d.

We demonstrated that the N-CB catalyst incorporated carbon felt electrode dramatically improve the electrochemical performance of the VRFB system. These exceptional electrochemical properties can be attributed to the surface functionalized carbon black synthesized by corn protein self-assembly. The conductive and continuous graphitic coating layer of N-CB catalyst, as well as its high surface areas with surface oxygen and nitrogen functional groups helps to improve the electrocatalytic activities for the vanadium redox reaction.

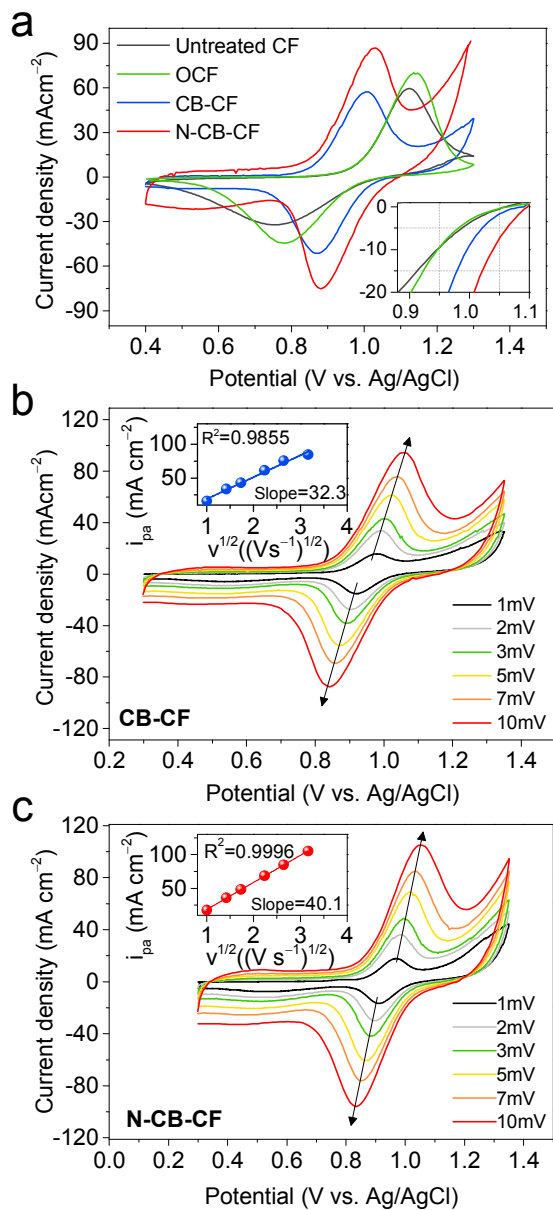


Figure 5. a) Cyclic voltammograms (CVs) of the untreated, oxidized, CB, and N-CB carbon felt at a scan rate of 5 mV s⁻¹ with potential window of 0.4 to 1.3 V versus Ag/AgCl. b) CVs of the N-CB carbon felt at different scan rates. Inset: plot of the anodic peak current (I_{pa}) versus the square root of each scan rate. CF: Carbon felt

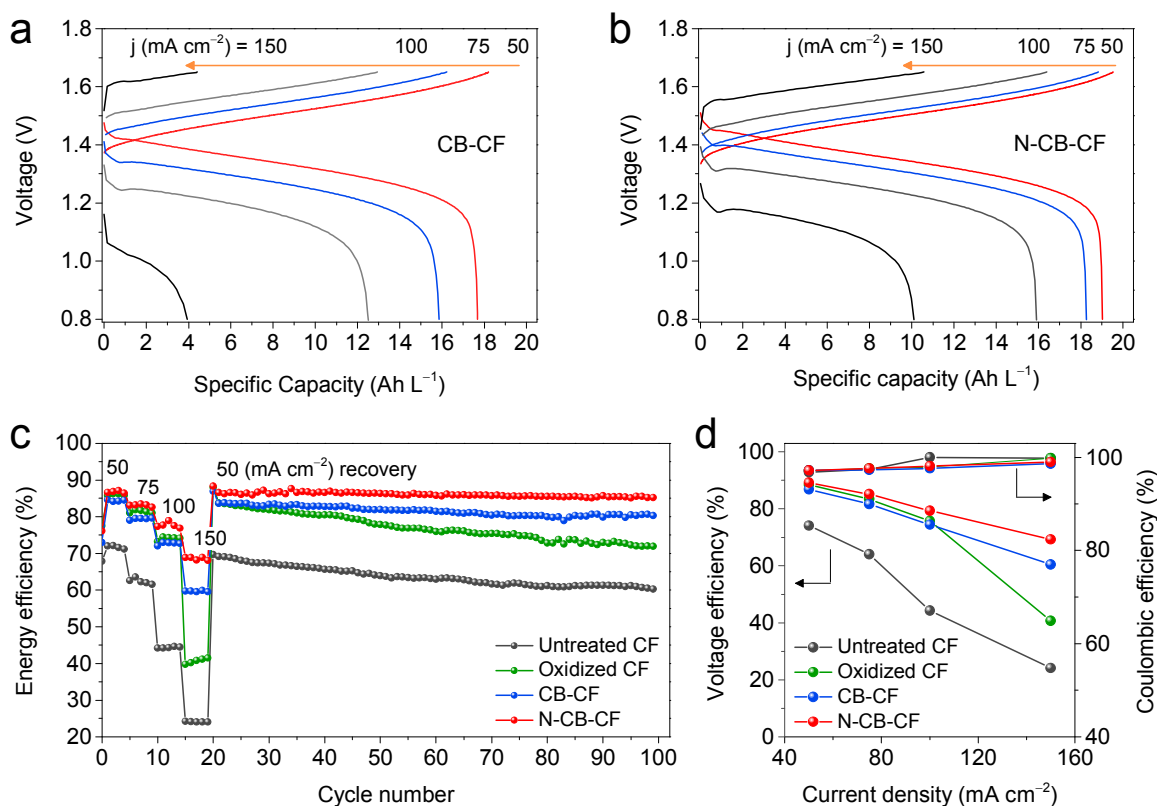


Figure 6. a) Electrochemical cycling performance of the untreated, oxidized, CB, and N-CB carbon felt electrode, and b) their Voltage efficiency and Coulombic efficiency during the rate capability test. CF: carbon felt

To elucidate the surface redox reaction mechanism, the oxidized carbon felt thermally activated at 500 °C for 5 h in air atmosphere was used as the control electrode in the identical flow battery cell. The experimental results of the oxidized carbon felt were obtained and compared to those of the N-CB carbon felt electrode as shown in the Figure 7. Figure 7a presents that the atomic content ratio of oxygen to carbon atom in the oxidized carbon felt electrode is ca. 0.22 that is two times higher than that of the N-CB carbon felt sample (ca. 0.10). This control electrode with high oxygen contents can be expected to provide much more vanadium active sites. The improved redox current peak of oxidized carbon felt electrode compared with that of the low oxygen containing CB carbon felt was confirmed in the cyclic voltammogram (Figure 5a). Further, the cycle performance test of the oxidized carbon felt (Figure 7b) shows the increased discharge capacity at an initial stage due to the abundant oxygen functional groups. However, there is no apparent capacity improvement at higher charge/discharge current rate for the oxidized carbon felt sample because of the lowered electron conductivity. This may be caused by the excessive surface functional groups of the oxidized carbon felt, which leads to the increase of cell overpotentials. In contrast, the carbon felt coated with the carbon black, known as a conductive carbon composed of a large amount of sp² hybridized carbon (C=C), successfully presented the capacity retentions even at higher current densities, but it showed a low capacity retention. This low capacity is mainly caused by the insufficient surface active sites for the vanadium redox reaction on the CB carbon felt electrode with the low the O/C ratio of ca. 0.02. This result is also consistent with the cyclic voltammetry test. It is worth mentioning that the balance

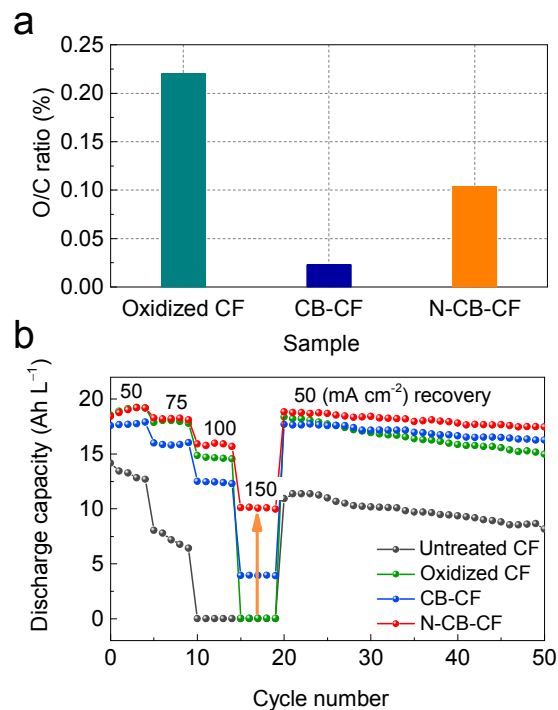


Figure 7. a) Chemical composition ratio of oxygen and carbon atoms for oxidized, CB, and N-CB carbon felt electrodes. And b) Discharge cycling performance

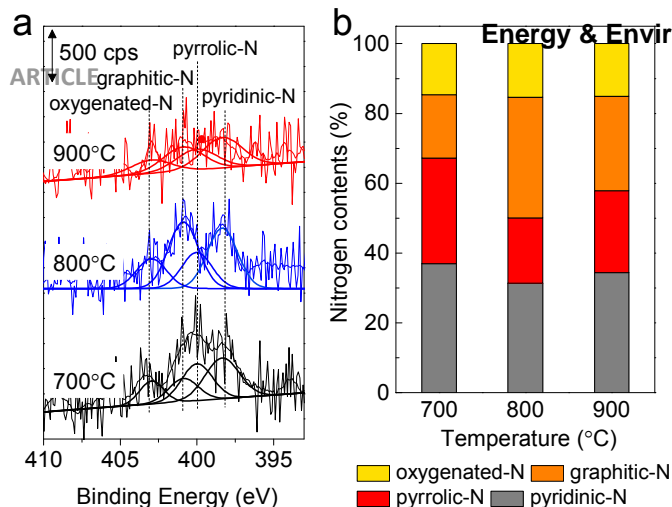


Figure 8. a) Ex-situ XPS analysis of N-CB catalyst prepared at various temperatures (700, 800, and 900 °C) and b) its chemical composition ratio of N1s spectra.

between the surface vanadium active sites (toward V^{2+}/V^{3+} and VO^{2+}/VO_2^+ ions) and the electron conductivity may be of importance for developing high performance electrocatalysts in the VRFB systems. Thus, the N-CB catalyst can be one of the ideal electrocatalysts for the high-performance flow battery system due to its high surface areas with an oxygen-rich (content of ca. 10 wt%) and N-doped coating layer. It exhibited the significant improvement of battery performance evident from the cyclic voltammograms and battery cycling tests.

In addition, the N-doping into carbon materials has been found to promote vanadium redox reactions by high negatively charged electron density of the incorporated nitrogen atom.²³ Accordingly, the doped nitrogen atoms as a defect site originated from the zein protein could create a lone pair of electron localized states in carbon black surface. This eventually facilitates the electron transfer and vanadium ions adsorption steps, resulting in high rate capability at 150 mA cm^{-2} and stable capacity retentions. In addition, the origin of catalytic activity among four different nitrogen species was examined by high-resolution N1s spectra (Figure 8) and cyclic voltammograms (Figure S7b). Compared with the relation between the content of each nitrogen species and the electrochemical catalytic activity, it was proportional to the content of a graphitic (quaternary) nitrogen, centered for 401.1 eV. Such results are consistent with the previous studies reporting that the graphitic nitrogen is highly stable in an acidic condition and less susceptible to protonization.²³ Therefore, we can reasonably conclude that the stable nitrogen defects on the N-CB catalyst play an important role to efficiently promote the adsorption of vanadium redox couples.

Conclusion

In summary, we developed the highly efficient carbon-based electrocatalyst for high-performance VRFBs by an inexpensive, environmentally friendly, and safe synthesis methods. The amphiphilic properties of the zein protein enabled it to have the self-assembly on the CB nanoparticles by the EISA process, which led to coating the N-doped coating layer on the CB nanoparticles. As a result, the N-CB has high surface areas with the abundant oxygen functional groups and N-doped coating networks for the vanadium active sites and high electron conductivity. Compared with the CB catalyst, the N-CB catalyst exhibited the excellent catalytic activity towards vanadium redox reactions due to its oxygen-rich high surface

areas and nitrogen functionality for enhanced electron transfer rate and faster vanadium ion transfer kinetics.

Acknowledgements

This research was supported by MSIP (Ministry of Science, ICT&Future Planning), Korea, under the C-ITRC (Convergence Information Technology Research Center) support program (NIPA-2013-H0301-13-1009) supervised by the NIPA (National IT Industry Promotion Agency).

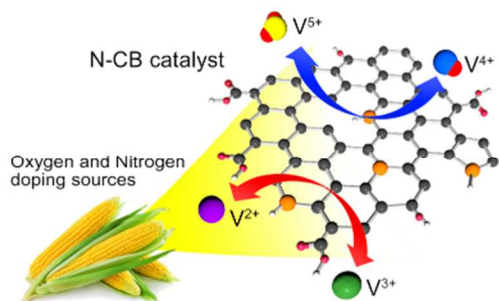
References

- Z. Yang, J. Zhang, M. C. Kintner-Meyer, X. Lu, D. Choi, J. P. Lemmon and J. Liu, *Chem. Rev.*, 2011, 111, 3577-3613.
- J. Liu, J.-G. Zhang, Z. Yang, J. P. Lemmon, C. Imhoff, G. L. Graff, L. Li, J. Hu, C. Wang, J. Xiao, G. Xia, V. V. Viswanathan, S. Baskaran, V. Sprenkle, X. Li, Y. Shao and B. Schwenzer, *Adv. Funct. Mater.*, 2013, 23, 929-946.
- Y. Zhao, M. Hong, N. Bonnet Mercier, G. Yu, H. C. Choi and H. R. Byon, *Nano Lett.*, 2014, 14, 1085-1092.
- B. Huskinson, M. P. Marshak, C. Suh, S. Er, M. R. Gerhardt, C. J. Galvin, X. Chen, A. Aspuru-Guzik, R. G. Gordon and M. J. Aziz, *Nature*, 2014, 505, 195-198.
- B. Dunn, H. Kamath and J. M. Tarascon, *Science*, 2011, 334, 928-935.
- Q. Liu, A. Turhan, T. A. Zawodzinski and M. M. Mench, *Chem. Commun.*, 2013, 49, 6292-6294.
- B. Li, M. Gu, Z. Nie, Y. Shao, Q. Luo, X. Wei, X. Li, J. Xiao, C. Wang, V. Sprenkle and W. Wang, *Nano Lett.*, 2013, 13, 1330-1335.
- K. J. Kim, Y.-J. Kim, J.-H. Kim and M.-S. Park, *Mater. Chem. Phys.*, 2011, 131, 547-553.
- C. Ding, H. Zhang, X. Li, T. Liu and F. Xing, *J. Phys. Chem. Lett.*, 2013, 4, 1281-1294.
- B. Sun and M. Skyllas-Kazacos, *Electrochim. Acta*, 1992, 37, 2459-2465.
- W. Wang, Q. Luo, B. Li, X. Wei, L. Li and Z. Yang, *Adv. Funct. Mater.*, 2013, 23, 970-986.
- G. J. Wei, C. K. Jia, J. G. Liu and C. W. Yan, *J. Power Sources*, 2012, 220, 185-192.
- L. Yue, W. S. Li, F. Q. Sun, L. Z. Zhao and L. D. Xing, *Carbon*, 2010, 48, 3079-3090.
- S. Wang, X. Zhao, T. Cochell and A. Manthiram, *J. Phys. Chem. Lett.*, 2012, 3, 2164-2167.
- C. A. Yao, H. M. Zhang, T. Liu, X. F. Li and Z. H. Liu, *J. Power Sources*, 2012, 218, 455-461.
- K. J. Kim, M. S. Park, J. H. Kim, U. Hwang, N. J. Lee, G. Jeong and Y. J. Kim, *Chem. Commun.*, 2012, 48, 5455-5457.
- W. H. Wang and X. D. Wang, *Electrochim. Acta*, 2007, 52, 6755-6762.
- T. M. Tseng, R. H. Huang, C. Y. Huang, K. L. Hsueh and F. S. Shieu, *J. Electrochem. Soc.*, 2013, 160, A690-A696.
- Z. González, A. Sánchez, C. Blanco, M. Granda, R. Menéndez and R. Santamaría, *Electrochem. Commun.*, 2011, 13, 1379-1382.
- B. Li, M. Gu, Z. Nie, X. Wei, C. Wang, V. Sprenkle and W. Wang, *Nano Lett.*, 2014, 14, 158-165.
- P. X. Han, Y. H. Yue, Z. H. Liu, W. Xu, L. X. Zhang, H. X. Xu, S. M. Dong and G. L. Cui, *Energy Environ. Sci.*, 2011, 4, 4710-4717.
- M. Park, Y. J. Jung, J. Kim, H. I. Lee and J. Cho, *Nano Lett.*, 2013, 13, 4833-4839.
- J. Jin, X. Fu, Q. Liu, Y. Liu, Z. Wei, K. Niu and J. Zhang, *ACS Nano*, 2013, 7, 4764-4773.
- Y. Shao, X. Wang, M. Engelhard, C. Wang, S. Dai, J. Liu, Z. Yang and Y. Lin, *J. Power Sources*, 2010, 195, 4375-4379.
- D. Oh, J. Qi, Y. C. Lu, Y. Zhang, Y. Shao-Horn and A. M. Belcher, *Nat. Commun.*, 2013, 4, 2756.
- Y. Zhao, F. Sakai, L. Su, Y. Liu, K. Wei, G. Chen and M. Jiang, *Adv. Mater.*, 2013, 25, 5215-5256.

27. Z. G. Wang and B. Ding, *Adv. Mater.*, 2013, 25, 3905-3914.
28. X. Y. Chen, C. Chen, Z. J. Zhang and D. H. Xie, *J. Mater. Chem. A*, 2013, 1, 10903.
29. H. Zhu, J. Yin, X. Wang, H. Wang and X. Yang, *Adv. Funct. Mater.*, 2013, 23, 1305-1312.
30. C. H. Choi, S. H. Park and S. I. Woo, *Green Chem.*, 2011, 13, 406.
31. J. Luecha, A. Hsiao, S. Brodsky, G. L. Liu and J. L. Kokini, *Lab. Chip.*, 2011, 11, 3419-3425.
32. J. W. Lawton, *Cereal Chem.*, 2002, 79, 1-18.
33. Y. Wang and G. W. Padua, *Langmuir*, 2010, 26, 12897-12901.
34. N. Matsushima, G.-i. Danno, H. Takezawa and Y. Izumi, *Biochim. Biophys.*, 1997, 1339, 14-22.
35. P. Argos, K. Pedersen, M. D. Marks and B. A. Larkins, *J. Biol. Chem.*, 1982, 257, 9984-9990.
36. Y. Wang and G. W. Padua, *Langmuir*, 2012, 28, 2429-2435.
37. A. C. Ferrari and D. M. Basko, *Nat. Nanotechnol.*, 2013, 8, 235-246.
38. Y. Li, W. Zhou, H. Wang, L. Xie, Y. Liang, F. Wei, J. C. Idrobo, S. J. Pennycook and H. Dai, *Nat. Nanotechnol.*, 2012, 7, 394-400.
39. W. Li, J. Liu and C. Yan, *Electrochim. Acta*, 2011, 56, 5290-5294.
40. K. Gong, F. Du, Z. Xia, M. Durstock and L. Dai, *Science*, 2009, 323, 760-764.
41. R. H. Huang, C. H. Sun, T. m. Tseng, W. k. Chao, K. L. Hsueh and F. S. Shieu, *J. Electrochem. Soc.*, 2012, 159, A1579-A1586.

TOC figure

Corn protein-derived nitrogen-doped carbon nanomaterial was fabricated, which has abundant oxygen active sites and nitrogen defects for vanadium redox reactions.



(6.75 cm X 4 cm)